energies

MDPI

Article

Research on Microwave Non-Destructive Testing Method for Defects in 10 kV Distribution Cable Intermediate Joints

Wangjun Deng [1], Li Cheng [1,*], Xiying Wang [2], Hao Luo [1] and Tengyi Zhang [1]

[1] School of Electrical Engineering, Chongqing University, Chongqing 400044, China; dengwangjun@stu.cqu.edu.cn (W.D.); haoluo@cqu.edu.cn (H.L.); zhangty174@163.com (T.Z.)
[2] Yunnan Electric Power Dispatch and Control Center, Kunming 650011, China; 18535965807@163.com
* Correspondence: chengl16@cqu.edu.cn; Tel.: +86-023-65102434

Abstract

This study aims to propose a defect diagnosis method for distribution cable intermediate joints based on microwave reflection. The research focuses on 10 kV cold-shrink-type distribution cable intermediate joints, employing both simulation analysis and experimental methods. Firstly, a microwave defect detection model for intermediate joints is derived. CST simulations are conducted to analyze the variation of the reflection coefficient (S_{11}) under different detection frequencies, defect depths, and defect types. Next, flat plate and real prototype samples of intermediate joints with defects such as insulation scratches, conductive impurities, and moisture ingress are fabricated. A microwave reflection detection platform is established to test the artificially defective samples. Reflection voltage signals corresponding to different defects are obtained. The concept of the relative value of the reflection voltage difference is then introduced, resulting in significant changes in the detection results, which effectively indicate the presence of different defects. Finally, the reflection voltage signals under different defect sizes, silicone rubber thicknesses, detection distances, and detection angles are studied. The results show that this method is capable of detecting defects as small as 2 mm in width and 0.2 mm in depth. The silicone rubber thickness, detection distance, and detection angle significantly affect the detection results. This demonstrates that microwave reflection signals can effectively identify the type and severity of defects within cable intermediate joints, and the method can be extended to detect internal defects in other layered composite insulation structures.

Keywords: cable intermediate joint; composite insulation structure; microwave reflection; defect identification; non-destructive testing (NDT)

Academic Editor: Constantinos S. Psomopoulos

Received: 27 November 2025
Revised: 13 January 2026
Accepted: 16 January 2026
Published: 19 January 2026

1. Introduction

The 10 kV cable intermediate joint is a key component in the power cable system, primarily used to connect two sections of cable or repair damaged parts, ensuring the continuity and reliability of power transmission [1]. The cable intermediate joint has a multi-layer composite insulation structure. Due to the compact design and the complex manufacturing and installation processes, defects of varying degrees are likely to occur within the insulation layers. Since the dielectric strength that each layer in the multi-layer composite insulation structure can withstand is proportional to the corresponding electrical strength, once the field strength exceeds the tolerance of a given dielectric layer, that layer will break down, and it can easily lead to breakdown of other dielectric layers [2]. In non-uniform electric fields or under small overvoltage conditions, a "cumulative effect" will occur, causing a decrease in the breakdown voltage of solid dielectric materials, which then leads to partial discharge. Over time, this can lead to the degradation of the insulation performance of the intermediate joint, and in severe cases, it can cause insulation breakdown [3–5]. Therefore, using non-destructive testing (NDT) technology to detect and evaluate defects in cable intermediate joints is of great importance [6].

Currently, the main non-destructive testing methods for detecting defects in cable intermediate joints include partial discharge detection, ultrasonic testing, infrared imaging detection, X-ray/CT testing, and acoustic detection [7–17]. Partial discharge detection assesses the insulation condition by monitoring partial discharge signals from the cable intermediate joint under high voltage. However, it is susceptible to electromagnetic interference and requires shielding to block environmental noise [8–12]; ultrasonic testing detects internal defects or interface pressure changes by analyzing the propagation characteristics of ultrasonic waves in materials (reflection, refraction, attenuation, etc.). It requires coupling agents (such as glycerin) to transmit ultrasonic waves and cannot be used in a vacuum [13,14]; infrared imaging detection identifies local overheating or insulation degradation areas by measuring the temperature distribution on the surface of the cable intermediate joint. However, it is sensitive to environmental temperature and radiation interference, and can only detect surface or near-surface defects, being insensitive to deep defects [15]; X-ray/CT testing uses X-rays to penetrate materials and analyzes internal structural defects through imaging. However, the equipment is costly, and there is a risk of radiation exposure, requiring strict safety precautions. It also has low sensitivity for materials with small density differences (such as rubber–polyethylene interfaces) [16]; acoustic detection analyzes fault characteristics by collecting sound signals (such as discharges and mechanical vibrations) from cable accessories during operation. However, environmental noise can affect the accuracy of detection [17]. In summary, there is an urgent need for a method capable of identifying and detecting defects inside cable joints.

Microwave testing technology, as a new non-destructive testing method, has the advantages of high sensitivity to non-metallic materials, non-contact detection, no coupling agents required, high resolution, and adjustable safety [18–20]. Currently, there has been a large amount of research on microwave non-destructive testing technology worldwide, but research on its application to cable intermediate joint detection is still limited. Wang Xujie et al. proposed a method for detecting steel rebar corrosion in reinforced concrete structures based on microwave reflection. They used CST Studio Suite 2021 3D electromagnetic simulation software to establish a numerical simulation model of corrosion in reinforced concrete structures. By analyzing the changes in echo loss, they revealed the impact of different corrosion degrees on microwave testing results [21]. Wang Liming et al. used the reflection characteristics of microwaves at the interface between different insulation layers to detect defects. They conducted experiments using flat samples and studied the relationship between defect size and detection accuracy. In the experiments, defects as small as 0.3 mm deep and 4 mm wide within the flat sample were detectable [22,23].

This paper proposes a microwave non-destructive testing method for detecting defects in 10 kV distribution cable intermediate joints. It uses simulation models to detect defects of different depths and types in intermediate joints, and experimental results are provided to verify the effectiveness of the proposed method in detecting defects in intermediate joints.

2. Model Construction

This paper uses the wave impedance model to calculate the reflection coefficient. The process of microwave inspection of the intermediate joint is simplified into the structure shown in Figure 1.

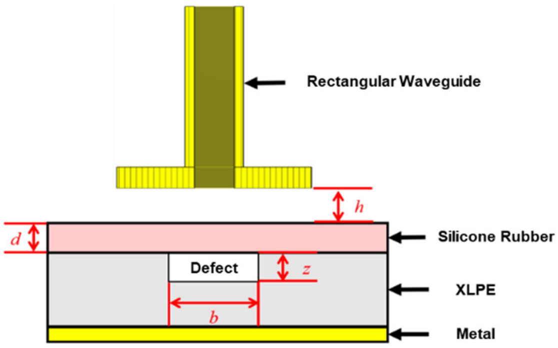

Figure 1. Microwave Inspection Model of Defects in the Intermediate Joint.

The intermediate joint is simplified into a planar structure consisting of a silicone rubber layer, a cross-linked polyethylene (XLPE) layer, and a metal layer. The detection probe is a metal waveguide with a rectangular cross-section. The dielectric constant ε, magnetic permeability μ, and thickness d of each layer of the medium are considered.

The wave impedance characterizes the ability of a medium to propagate electromagnetic waves. The reflection and refraction coefficients at the interface between two media can be calculated from the wave impedances of the two media. According to transmission line theory, for two planar media, the transmission line can be equivalently represented by a single new medium, and the new wave impedance is defined as the equivalent wave impedance.

$$\eta_{ef} = \eta_1 \frac{\eta_2 - \mathrm{j}\eta_1 \tan(k_1 D)}{\eta_1 - \mathrm{j}\eta_2 \tan(k_1 D)} \tag{1}$$

Here, k is the wave number. A phase change of 2π in space corresponds to one full wave, and k represents the number of full waves per unit length.

$$k = \omega\sqrt{\mu\varepsilon} \tag{2}$$

μ and ε are the magnetic permeability and dielectric constant of the medium. D is the thickness of the incident medium; η_1 and η_2 are the wave impedances of the materials on the incident and transmission sides of the medium, respectively.

$$\eta = \sqrt{\frac{\mu}{\varepsilon}} \tag{3}$$

For multi-layer media, the bottom two layers of the medium are equivalently represented as a single wave impedance, effectively reducing the total number of medium layers by one. In other words, by repeatedly using Formula (1) and calculating from the transmission end to the incident end, the overall wave impedance can be obtained.

A rectangular waveguide is also a type of transmission line for electromagnetic waves, and its wave impedance is [24]:

$$\eta_{rw} = 2\frac{b}{a}\sqrt{\frac{\mu}{\varepsilon}}\frac{1}{\sqrt{1-(\lambda/2a)^2}} \tag{4}$$

where a and b are the length and width of the cross-section of the rectangular waveguide, and λ is the operating microwave wavelength.

According to the wave impedance theory, the waveguide and the test sample are considered as two separate transmission lines. The reflection coefficient R at their interface is:

$$R = \frac{\eta_{rw} - \eta_{ef}}{\eta_{rw} + \eta_{ef}} \tag{5}$$

By calculating with Formula (5), it can be observed that when there is a defect in the intermediate joint (such as air gaps, the presence of conductive impurities, or moisture), the reflection coefficient of the microwaves at the interface between the waveguide probe and the intermediate joint will change significantly. This, in turn, causes a noticeable variation in the reflected signal. Based on this principle, internal defects in the intermediate joint can be detected by monitoring changes in the reflected signal's amplitude.

3. Materials and Methods

3.1. Software Simulation

Based on the actual dimensions of the 10 kV cold shrink cable joint for the studied model, a model was created in CST STUDIO SUITE, and material properties were assigned. Frequency variations influence the relative permittivity of materials; however, due to experimental constraints during the current research process, the relative permittivity of various materials within the cable joint at frequencies between 25 GHz and 30 GHz has yet to be measured. In this study, relative permittivity parameters measured at 50 Hz were employed for simulation analysis. This simulation served solely to confirm the overall sensitivity of the S_{11} parameter to defect type, defect location, defect depth, and other parameters detailed in the paper. The material properties for each structure are shown in Table 1.

Table 1. Parameters of the Mediums in the Cable Joint.

Material	Relative Dielectric Constant (ε)	Thickness (d/mm)
Silicone Rubber	3.2	2
XLPE (Cross-linked Polyethylene)	2.25	5
Conductor Shielding Layer/Insulation Shielding Layer	2.3	/
Shielding Tube	700	/
Stress Cone	40	/
Outer Shielding	20	/
Waterproof Insulation Tape	3	/
Semiconductive Tape	10	/
Air	1.00059	0.5
Copper Conductor	/	0.5
Water	78	0.5

Build a Model for the 10 kV Cold Shrink Cable Joint Based on the Parameters Above and Conduct a Simulation Experiment, as Shown in Figure 2.

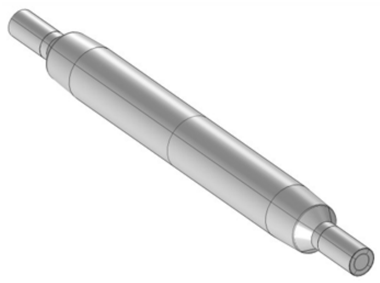

Figure 2. 10 kV Cold Shrink Cable Joint Model.

The S_{11} parameter is the input reflection coefficient, which is used to describe the reflection of the signal at the input port. This paper focuses on observing the variation of the reflection coefficient S_{11} based on the reflection characteristics of defects in the cable joint, in order to determine the type and location of the defect. To improve the accuracy and sensitivity of detection, S_{11} is quantified in logarithmic form during the experiment, with its unit in decibels (dB).

$$S_{11} = 20\lg|S_{11}| \quad (6)$$

3.2. Sample Preparation

Considering the complex structure of the cable joint, which makes it difficult to perform microwave testing on the entire joint, a simplified 3-layer composite structure is used to simulate the actual cable joint, as shown in Figure 3a. Based on the principle of structural equivalence, the simplified 3-layer composite material is structurally similar to the actual cable joint and is consistent with the detection principle.

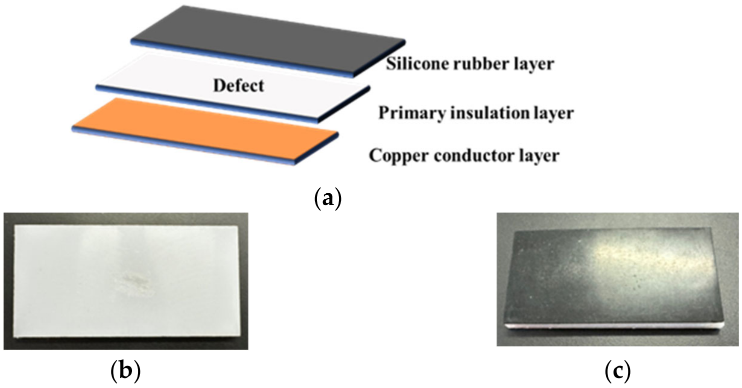

Figure 3. Cable Joint Flat Sample. (**a**) Schematic Diagram of the Cable Joint Flat Sample; (**b**) XLPE After Destruction by Electric Grinder; (**c**) Flat Sample.

Based on the above equivalent simplified structure, defect-containing three-layer composite insulation samples were prefabricated in the laboratory, as shown in Figure 1. From top to bottom, the first layer is the silicone rubber layer, with dimensions of 100 mm × 50 mm × 3 mm; the second layer is the cross-linked polyethylene (XLPE) layer, with dimensions of 100 mm × 50 mm × 3 mm; and the third layer is the copper conductor layer, with dimensions of 100 mm × 50 mm × 1 mm. Since microwaves undergo total reflection when encountering metal, the thickness of the copper plate has no impact on the detection results, so it is set to 1 mm. To closely replicate typical internal defects in cable joints, local defects such as main insulation scratches, mixed metal conductive impurities, and moisture absorption were simulated. The XLPE insulation sample was damaged with an electric grinder, and artificial defects were pre-fabricated at the damaged locations. The specific pre-fabrication methods are as follows: an electric grinder was used to grind a shallow rectangular groove, simulating an air gap defect; copper foil was applied to the XLPE layer, simulating conductive impurity defects; and water-saturated absorbent paper was placed on the XLPE, simulating moisture ingress defects. Finally, the three layers of material were bonded with adhesive, and microwave testing was conducted, as shown in Figure 3b,c.

To ensure the accuracy of the experiment, a 10 kV XLPE distribution cable cold-shrink-type joint was selected. The same method was used to simulate defects, followed by testing, as shown in Figure 4.

Figure 4. 10 kV Cold-Shrink Cable Joint Sample.

3.3. Test Platform

To measure the microwave reflection signal characteristics of different defects in the cable joint, a reflective microwave detection system was constructed in this study. The system mainly includes a microwave signal source, power amplifier, rectangular waveguide, directional coupler, detector, data acquisition card, and computer. Due to the frequency range of the measurement system being 25 GHz to 30 GHz, the selected rectangular waveguide model is BJ260 (Xi'an Hengda Microwave Technology Development Co., Ltd., Xi'an, China), with an internal cross-sectional dimension of 8.636 mm × 4.318 mm, and the dominant mode operating frequency is 21.7–33 GHz. The principle of the reflective microwave detection system is shown in Figure 5.

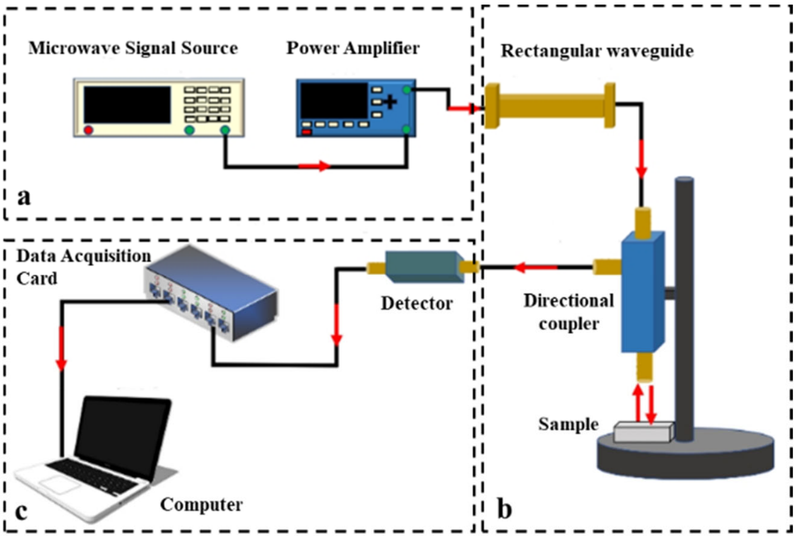

Figure 5. Reflective Microwave Detection System. (**a**) Generation of Microwaves; (**b**) Signal Detection System; (**c**) Signal Acquisition System.

Firstly, a microwave signal with adjustable frequency is generated by the microwave signal source. After amplification by the power amplifier, the microwave signal is transmitted through a rectangular waveguide. The signal enters the directional coupler's input, where it undergoes reflection and refraction at the cable joint sample. The reflected signal is separated by the directional coupler, and the detector converts the reflected signal into a DC voltage signal. The data acquisition card collects the DC voltage signal and sends it to the computer, where the upper-level program processes the data.

4. Simulation Analysis

4.1. Simulation Analysis of Different Frequencies and Defect Depths

In the CST software, set the simulation frequency range from 25 GHz to 30 GHz and the defect depth z from 0 mm to 2 mm, with a step size of 0.2 mm for the simulation analysis. The simulation results are shown in Figure 6.

From Figure 6, it can be seen that, within the frequency range of 25 GHz to 30 GHz, the reflection coefficient S_{11} for the defective cases is greater than that for the defect-free case (z = 0), and it increases as the defect depth increases. This variation is most noticeable around 28 GHz. The reflection coefficient S_{11} at this frequency is selected for further analysis, as shown in Figure 7.

From Figure 7, it can be observed that at a frequency of 28 GHz, as the defect depth increases, the reflection coefficient S_{11} shows a positive correlation with the defect depth, but the increase becomes slower and is not a linear relationship. This indicates that the microwave reflection detection method can detect defects at different depths in the middle joint of the cable.

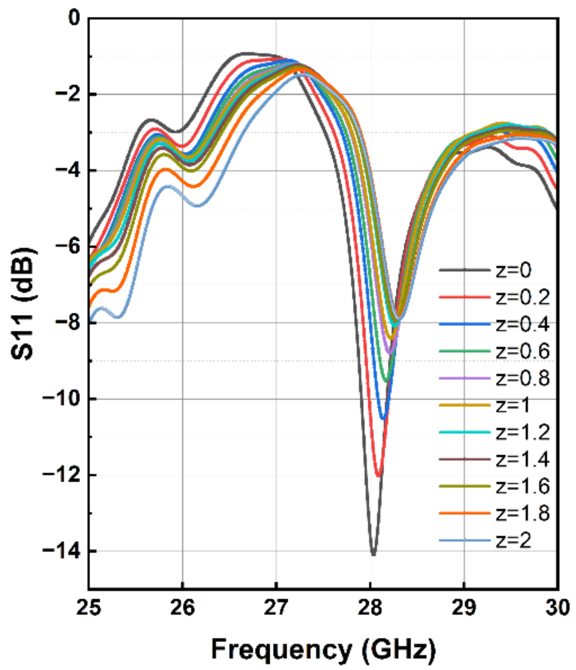

Figure 6. Reflection Coefficient S_{11} at Different Defect Depths.

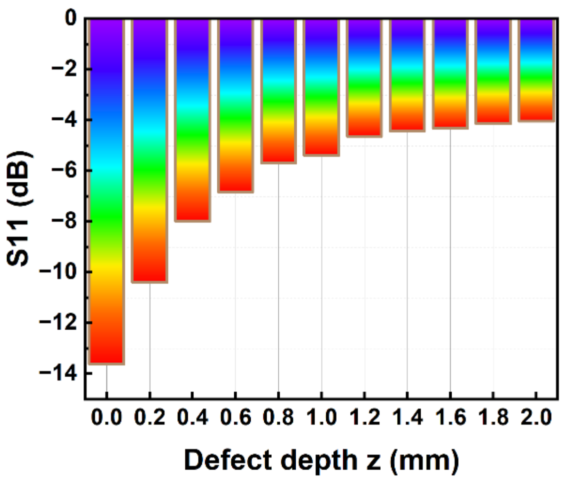

Figure 7. Reflection Coefficient S_{11} at Different Defect Depths at 28 GHz.

4.2. Simulation Analysis of Different Defect Types

In order to explore the trend of the microwave reflection coefficient S_{11} under different defect types, three types of defects were pre-formed on the surface of the XPLE: conductive impurities, main insulation scratches, and moisture. The dielectric materials at the defect locations were set as metal, air, and water, respectively. A rectangular waveguide was placed tightly against the surface, and simulation analysis was conducted at the previously mentioned frequency of 28 GHz. The simulation results are shown in Figure 8.

From Figure 8, it can be seen that the reflection coefficient S_{11} shows significant differences for different defect types, with the magnitudes in the following order: conductive impurity defect > air gap defect > no defect > moisture defect. The reflection coefficient is largest for the conductive impurity defect because microwaves undergo total reflection when encountering metal. The reflection coefficient is smallest for the moisture defect because microwaves are absorbed by water molecules. In summary, the variation in the magnitude of S_{11} can be used to identify different types of defects.

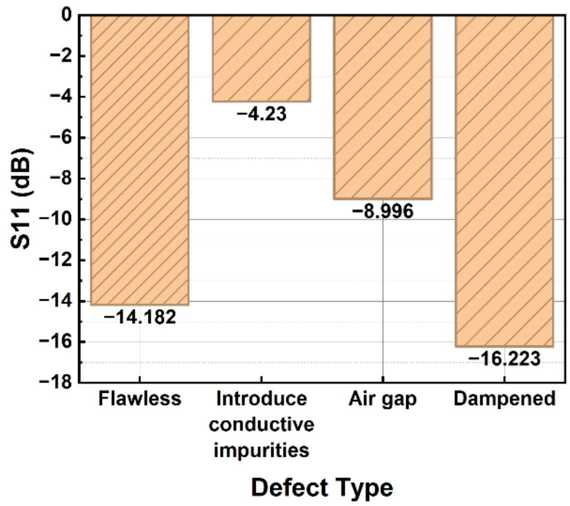

Figure 8. Reflection Coefficient S_{11} under Different Defect Types.

5. Experimental Results and Discussion

5.1. Selection of the Optimal Detection Frequency

The microwave signal source is adjustable within the frequency range of 25 GHz to 30 GHz. To achieve the best detection results, it is necessary to determine the reflected voltage signal from the sample at different frequencies, and then select the frequency corresponding to the optimal reflected voltage signal for subsequent experiments. A flat sample with a thickness of 3 mm for silicone rubber, 5 mm for XLPE, and 1 mm for copper sheet was selected for the experiment. The reflected voltage signals at different frequencies are shown in Figure 9.

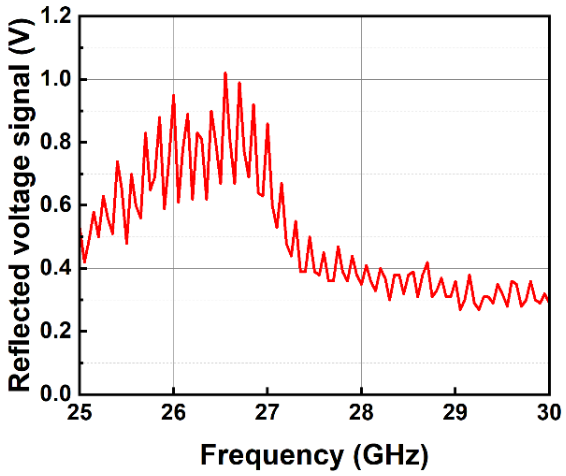

Figure 9. Reflected Voltage Signals of the Flat Sample at Different Frequencies.

It can be observed that the reflected voltage signal fluctuates with changes in frequency. This is due to the interference effect between the incident wave and the reflected wave generated at the points of impedance discontinuity within the system. The result of this interference is strongly dependent on the phase relationship between the two, with the phase difference being determined by both the propagation path length and the signal wavelength. When scanning the frequency, the change in wavelength leads to a continuous alteration of the phase difference, causing the interference state to periodically alternate between constructive and destructive interference. This ultimately results in a periodic fluctuation of the reflected signal in the frequency domain. At a frequency of 26.55 GHz, the reflected voltage signal reaches its maximum value of 1.05 V; thus this frequency is selected as the optimal detection frequency for subsequent experiments.

To maintain consistency with the actual intermediate joint, a 10 kV XLPE distribution cable cold-shrink-type intermediate joint was selected for the experiment. The reflected voltage signals at different frequencies are shown in Figure 10.

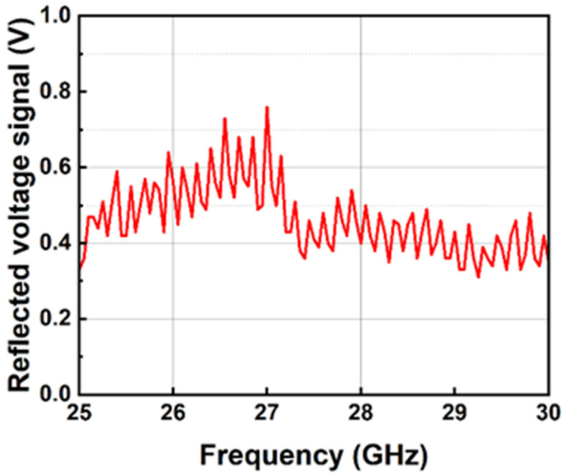

Figure 10. Reflected Voltage Signals of the Cold-Shrink-Type Intermediate Joint Sample at Different Frequencies.

It can be observed that the trend of the reflected voltage signal is similar to that of the flat sample, but the reflected voltage signal is smaller compared to the flat sample. This is due to the cylindrical shape of the cold-shrink-type intermediate joint, the incomplete fit between the rectangular waveguide port and the sample, and the structural characteristics of the sample. The maximum reflected voltage signal occurs at 27 GHz, with a value of 0.73 V. This frequency is selected as the optimal detection frequency for the cold-shrink-type intermediate joint sample in subsequent experiments.

5.2. The Reflected Signals of Different Defects

For the flat sample, microwave testing was first conducted on the pre-fabricated main insulation scratch defect, copper conductor impurity defect, and moisture defect. The test results are shown in Figure 11.

As shown in the figure, between detection points 1–10, the curves remain stable overall, with a noticeable change occurring only near detection point 6. In the absence of defects, the reflected signal is stable around 1.1 V, indicating low system noise and minimal signal fluctuation. For the main insulation scratch defect, there is a slight increase near detection point 6, reaching a peak of 1.32 V. The moisture defect shows a significant reflection attenuation at the same position, with the signal dropping to 0.23 V. The conductive impurity defect, on the other hand, exhibits the most prominent reflection peak, with an amplitude of 1.52 V.

It can be seen that different defect types have a significant impact on the reflected voltage signal: the conductive impurity defect causes the most severe impedance change, leading to a strong reflection signal; the moisture defect results in a weaker reflection signal due to increased dielectric polarization loss; while the main insulation scratch defect causes relatively minor impedance disturbance, resulting in a less noticeable reflection response.

Therefore, the reflection signal amplitude characteristics can be used to distinguish different types of defects, with the conductive impurity defect producing the strongest reflection signal, making it most sensitive to microwave reflection detection. The abnormal signal change at detection point 6 indicates the presence of a defect in that location, which can be used for pinpointing defect identification and type judgment in cables.

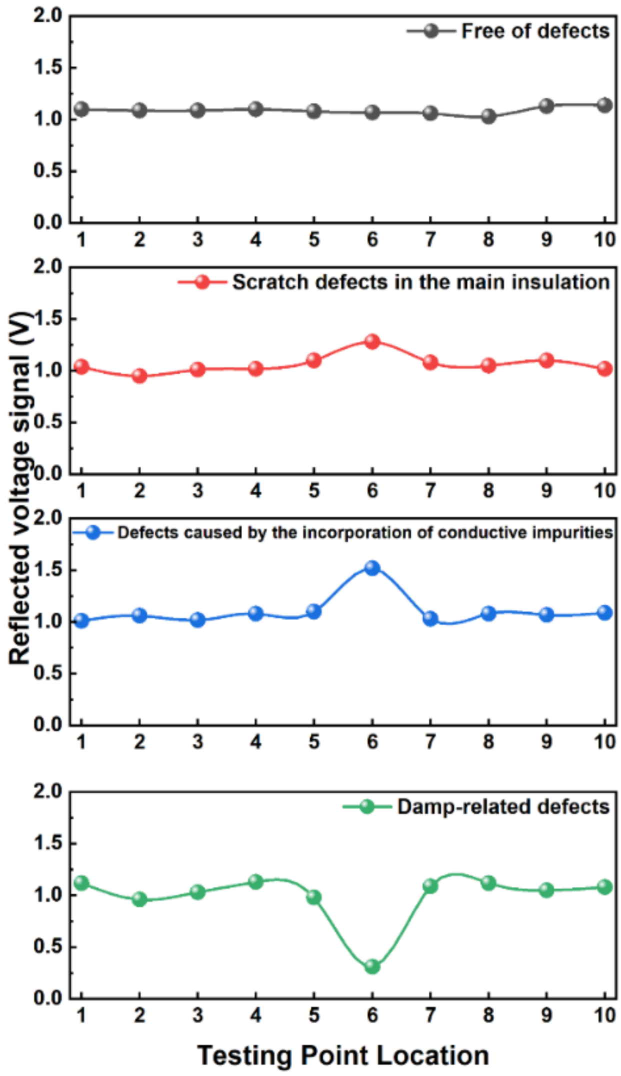

Figure 11. Reflected signals of different defects in the flat sample.

Next, defects similar to those in the flat sample were prefabricated in the cold-shrink intermediate joint sample, and the detection results are shown in Figure 12.

Compared to the flat sample, the reflected signal amplitudes in the cold-shrink intermediate joint sample are generally lower, with a reduced fluctuation range. This is due to the more complex structure of the intermediate joint, with multiple layers of dielectric materials. When microwaves propagate through these multi-layer dielectrics, they undergo multiple reflections and attenuations, which weakens the strength of the reflected signals. However, the variation trends are consistent between the two samples: different defect types show significant differences around detection point 6, with the conductive impurity defect having the largest reflection signal and the moisture defect showing the weakest reflection signal.

In conclusion, the microwave reflection method demonstrates good consistency between the detection results in both the flat sample and the cold-shrink intermediate joint sample. This verifies the feasibility and accuracy of the method in real cable joint structures, enabling precise defect localization and type identification.

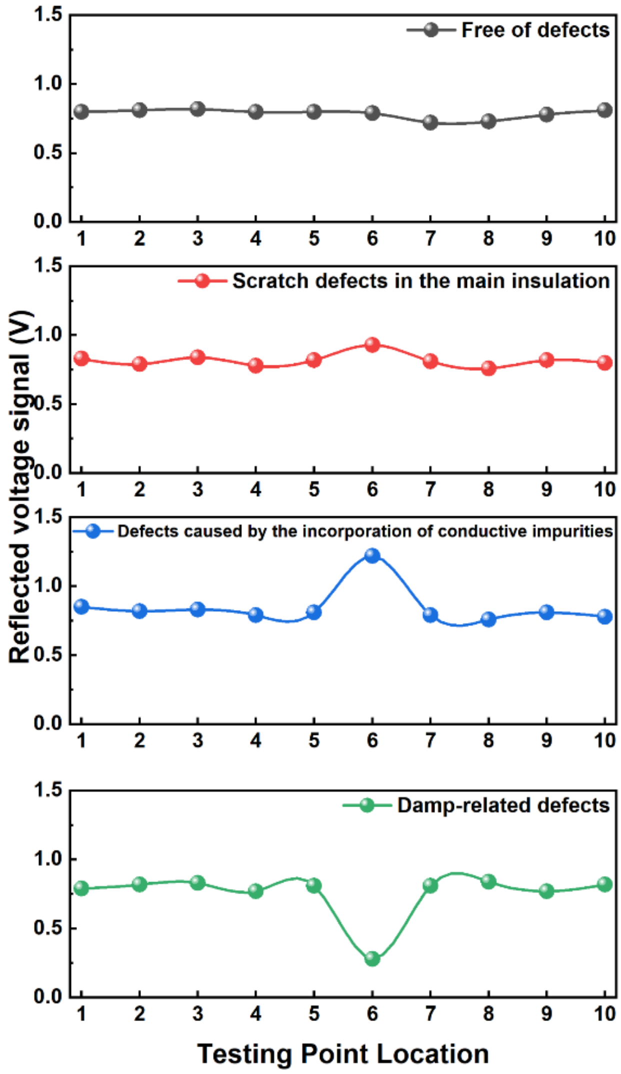

Figure 12. Reflected signals of different defects in the 10 kV cold-shrink cable intermediate joint sample.

5.3. Extraction and Analysis of Microwave Detection Signals

Due to the inability to ensure uniformity in material and thickness for each sample, and the difficulty in accurately controlling the detection distance and angle during the experiment, small variations may occur. Therefore, it is necessary to first calculate the system error for the defect-free flat sample and the defect-free cold-shrink intermediate joint sample. The system error U_e is the difference between the maximum and minimum values of the reflection voltage for the defect-free sample, as shown in expression (7). By comparing the actual measurement results with the system error, the internal defects of the cable terminal can be more accurately identified.

$$U_e = U_{max} - U_{min} \tag{7}$$

To more accurately identify defects, the reflection voltage signal U_i obtained from the detection is subtracted by the average reflection voltage U of the defect-free sample, resulting in the reflection voltage difference ΔU. The ratio of the reflection voltage difference ΔU to the system error U_e of the defect-free sample is then calculated, denoted as the relative value of the reflection voltage difference P_i, as shown in expression (8). If $P_i > 100\%$, it indicates that the reflection voltage difference exceeds the system error by more than one time, which is reflected as a noticeable change in the detection curve, allowing for effective determination of the presence of a defect.

$$P_i = \frac{U_i - \overline{U}}{U_e} \times 100\% = \frac{\Delta U}{U_e} \times 100\% \tag{8}$$

Three types of defects were pre-fabricated in the XLPE layer of the same flat sample. The length of the flat sample is 100 mm, denoted as y. At y = 20 mm, a main insulation scratch defect was pre-fabricated; at y = 50 mm, a conductive impurity defect was introduced; and at y = 80 mm, a moisture defect was created. Based on the relative value of the reflection voltage difference, the defect types were evaluated, and the results are shown in Figure 13.

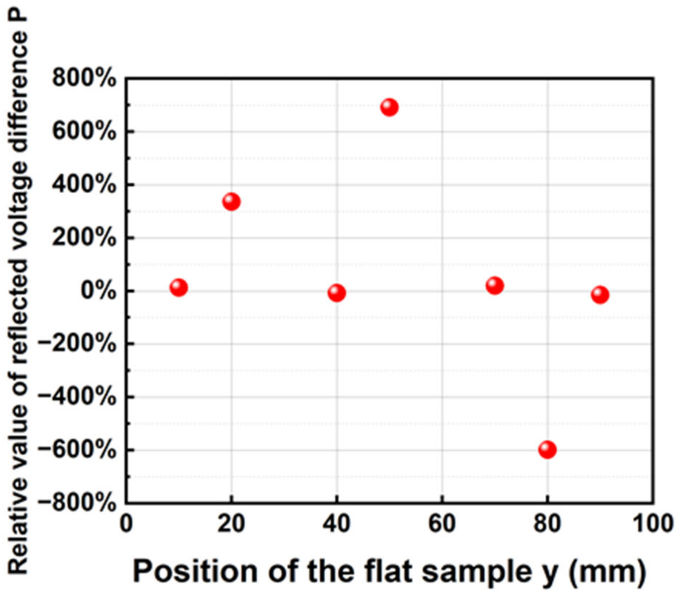

Figure 13. The relative values of the reflection voltage difference for different defects.

As shown in Figure 13, when three typical defects—main insulation scratch, conductive impurity, and moisture—were pre-fabricated in the XLPE layer of the same flat sample, the relative reflection voltage values P exhibited significant differences at different positions. Among them, the conductive impurity defect at y = 50 mm had the highest relative reflection voltage value, approximately +700%, indicating that the presence of conductive impurities significantly altered the electromagnetic properties of the local medium, resulting in the most noticeable impedance mismatch and the highest reflection energy. The main insulation scratch defect at y = 20 mm showed a relative reflection voltage value of approximately +300%, suggesting that although this defect damaged the integrity of the insulation layer, the reflection strength was relatively weak due to the material still being non-conductive. The moisture defect at y = 80 mm had a relative reflection voltage value of approximately −600%. This is because moisture has a high dielectric constant and loss characteristics, which causes absorption and phase inversion of the incident microwave signal, leading to a decrease in the reflection amplitude.

In summary, the impact of different types of defects on microwave reflection characteristics varies significantly. The reflection intensity decreases in the following order: conductive impurity defect > main insulation scratch defect > moisture defect. Therefore, the relative reflection voltage value can serve as an important characteristic parameter for determining the type of defect.

5.4. The Impact of Different Factors on Defect Detection

5.4.1. The Impact of Defect Size on Reflection Signals

Rectangular grooves with depths of 0.2 mm, 0.5 mm, 1 mm, 1.5 mm, and 2 mm, and widths of 2 mm, 4 mm, 6 mm, and 8 mm, and a length of 10 mm, were pre-fabricated at the center of the surface of different flat XLPE samples to simulate air gap defects of varying sizes. The experimental results are shown in Figure 14.

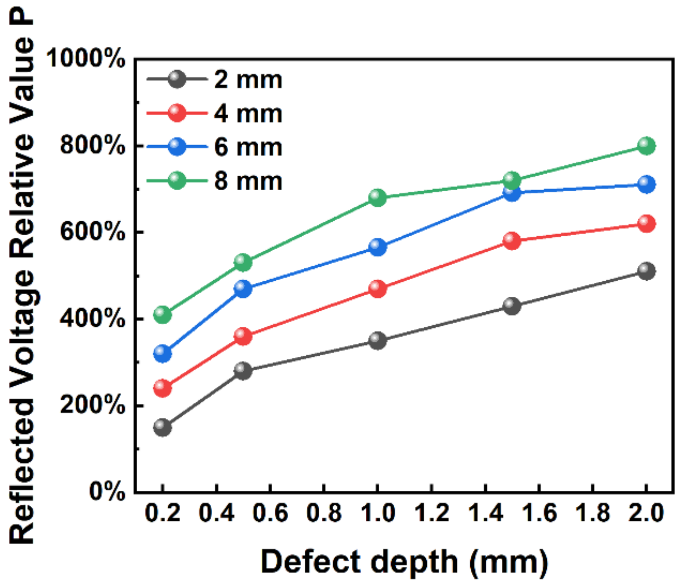

Figure 14. Reflection Voltage Difference Relative Value for Defects of Different Sizes.

From the chart, it can be observed that as the defect depth increases, the relative reflection voltage increases, regardless of the defect width. Additionally, at the same defect depth, the larger the defect width, the higher the relative reflection voltage. This indicates that both the defect depth and width have an impact on the relative reflection voltage. The deeper the defect and the wider the defect, the larger the relative reflection voltage, meaning that as the defect size increases, the detection effect becomes more apparent. This further verifies the feasibility of using microwave detection for the detection of defects of varying sizes.

5.4.2. The Impact of Different Silicone Rubber Thicknesses on Detection Results

Flat samples were selected, using silicone rubber plates of varying thicknesses ranging from 1 to 10 mm. One sample was created for each 1 mm increment in thickness. During testing, the waveguide probe was placed in close contact with the surface of the sample. For each sample, the reflection signal intensity at five different positions was measured, and the average value was taken. The experimental results are shown in Figure 15.

As shown in Figure 15, the reflection signal exhibits a distinct fluctuating trend with increasing thickness, rather than a nonlinear monotonic change. When the thickness is 2 mm, the reflection signal reaches its maximum value. A significant drop occurs in the range of 3–4 mm. As the thickness further increases, secondary peaks appear near 5 mm and 7 mm, respectively. When the thickness is increased to 9–10 mm, the reflection signal levels off and remains at a relatively low level.

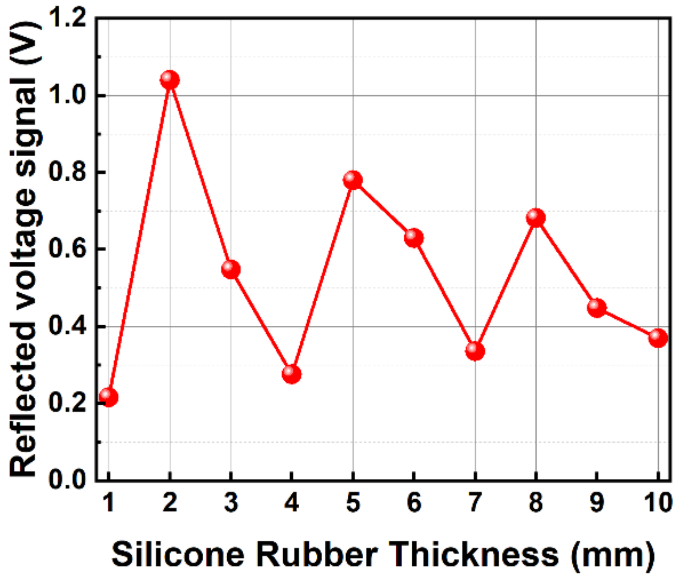

Figure 15. Reflection Voltage Signals at Different Silicone Rubber Thicknesses.

5.4.3. The Impact of Different Detection Distances on Detection Results

The flat sample with the optimal frequency from previous studies was selected to investigate the impact of detection distance h on the reflection voltage U. The detection distances h = 0 mm, 1 mm, 2 mm, 3 mm, 4 mm, 5 mm, 6 mm were tested. For each detection distance, experiments were conducted on the same defect-free flat sample. At each detection distance, reflection voltage U was randomly measured at 5 positions, and the average value was taken. The reflection voltage U at different detection distances h is shown in Figure 16.

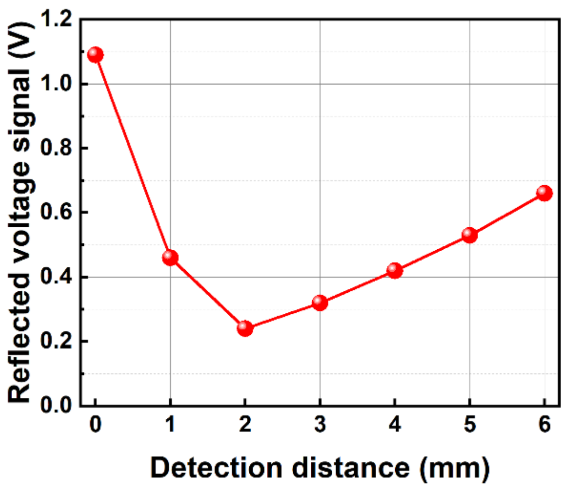

Figure 16. Reflection Voltage Signals at Different Detection Distances.

As shown in Figure 16, the reflection voltage exhibits a nonlinear trend of "rapid initial decrease, followed by gradual recovery" with the change in detection distance. When the probe is in close contact with the sample surface (h = 0), the near-field strong coupling results in the maximum reflection signal. As the detection distance increases to 1–2 mm, the coupling field strength rapidly attenuates, causing the reflection voltage to drop to its lowest value. When the detection distance further increases to 3–6 mm, the reflection path gradually transitions from near-field coupling mode to free-space propagation mode, resulting in a slight increase in reflection voltage. This result indicates that the microwave reflection method is highly sensitive to the detection distance, maintaining high energy coupling efficiency and defect identification sensitivity only within a small gap range. This characteristic is of significant reference value for the practical detection of cable joints in subsequent applications.

5.4.4. The Impact of Different Detection Angles on Detection Results

Since the detection relies on the intensity of reflected microwave signals, any variation in the sample's angle during the detection process can cause changes in the received reflection signal, leading to interference in the detection judgment. Therefore, it is necessary to study the relationship between the angle formed by the plane of contact between the sample and the probe (referred to as the detection angle) and the strength of the microwave reflection signal. As the angle is introduced, flat and cylindrical samples can no longer be well-equivalent, so a cold-shrinkable intermediate joint sample is used for the experiment.

As shown in Figure 17, the reflection voltage exhibits a distinct monotonic decrease with the increase in detection angle. When the detection angle is 0°, the probe is completely in contact with the joint surface, and the incident microwave aligns with the normal direction of the interface, resulting in the strongest near-field coupling and the highest reflection signal amplitude. As the detection angle gradually increases, the effective projection of the contact area decreases, the incident direction deviates from the normal, and the returning energy significantly attenuates, causing the reflection voltage to continuously decrease. At 5°, the reflection signal becomes very small compared to the initial value, indicating that even a slight angular deviation can have a significant impact on detection sensitivity. This result demonstrates that the detection angle is an important factor influencing the coupling efficiency between the waveguide aperture and the tested structure. When there is inclined incidence, part of the energy may propagate along the sheath surface or dissipate in the form of radiation, making it difficult to effectively couple back into the waveguide port, leading to a decrease in the apparent reflection coefficient. Therefore, in practical cable joint inspections, it is crucial to ensure that the probe maintains as close to normal incidence as possible with the joint's outer surface; otherwise, it will affect the distinguishability of defect reflection characteristics and the stability of the detection results.

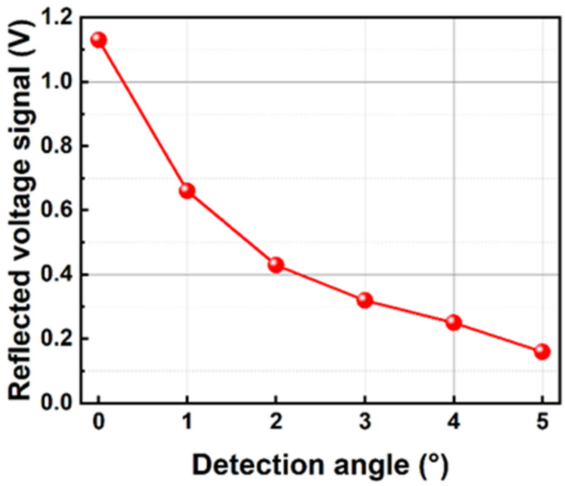

Figure 17. Reflection Voltage Signals at Different Detection Angles.

6. Conclusions

This paper proposes a defect detection method for 10 kV distribution cable intermediate joints based on microwave reflection. The method can sensitively identify various defects in the intermediate joint, enabling high-precision localization and severity diagnosis of the defects. The main conclusions obtained are as follows:

(1) Microwaves are highly sensitive to defects in the multi-layer composite insulation of cable intermediate joints. The microwave reflection signal can serve as a characteristic quantity for quickly identifying the types of internal defects.
(2) The reflection signal fluctuates with changes in microwave frequency. For the detection of different defects, the magnitude of the microwave reflection voltage signal is ranked as: conductive impurity defects > main insulation scratch defects > moisture defects. The relative value of the reflection voltage can be an important characteristic parameter for determining the type of defect in the sample.
(3) Both defect depth and width affect the relative value of the reflection voltage. The deeper and wider the defect, the larger the relative reflection voltage, i.e., the larger the defect size, the more apparent the detection effect. In the experiments, defects with a width of 2 mm and a depth of 0.2 mm were detected, further validating the feasibility of microwave detection for defects of different sizes.
(4) The reflection voltage signal shows periodic variation with different silicone rubber thicknesses and detection distances. In this study, the best detection effect was achieved when the silicone rubber thickness was 2 mm, and the rectangular waveguide aperture was in close contact with the sample surface. The reflection voltage was the highest when the detection angle was 0°, and it rapidly decreased as the detection angle increased.

The results of this study confirm that microwave reflection signals can effectively characterize the internal defects of the composite insulation structure in cable intermediate joints. Microwave detection can ultimately be used to provide early warning of the safety status of cable intermediate joints and other composite insulation structures.

Author Contributions: Methodology, W.D. and L.C.; Software, W.D.; Validation, W.D.; Formal analysis, W.D. and L.C.; Resources, X.W.; Data curation, W.D. and X.W.; Writing—original draft, W.D.; Writing—review & editing, L.C., H.L. and T.Z. All authors have read and agreed to the published version of the manuscript.

Funding: This research received no external funding.

Data Availability Statement: The datasets presented in this article are not readily available because [the data are part of an ongoing study or due to technical/time limitations]. Requests to access the datasets should be directed to [dengwangjun@stu.cqu.edu.cn].

Conflicts of Interest: Author Xiying Wang was employed by the company Yunnan Electric Power Dispatch and Control Center. The remaining authors declare that the research was conducted in the absence of any commercial or financial relationships that could be construed as a potential conflict of interest.

References

1. Zhang, Y.Y.; Jiang, F.Y.; Yu, X.Y.; Zhou, K.; Zhang, W.; Fu, Q.; Hao, J. Assessment of Thermal Aging Degree of 10kV Cross-Linked Polyethylene Cable Based on Depolarization Current. *IEEE Access* **2021**, *9*, 111020–111029. [CrossRef]
2. Wang, F.; Zhang, P.P.; Li, J.X.; Li, Z.Q.; Zhao, M.Z.; Liang, Y.L.; Su, G.Q.; You, X.H. Multi-feature based extreme learning machine identification model of incipient cable faults. *Front. Energy Res.* **2024**, *12*, 1364528. [CrossRef]
3. Tian, F.Q.; Li, X.B.; Zhang, S.T.; Cao, J.M. The Partial Discharge Evolution Characteristics of 10kV XLPE Cable Joint. *IEEE Access* **2023**, *11*, 108680–108687. [CrossRef]
4. Li, R.; Zhou, K.; Wan, H.; Xie, M.; Liu, L.; Wang, X.; Ma, X. Moisture Location of 10kV Cable Joints in Medium Voltage Distribution Grid Based on Frequency Domain Reflection. *Dianwang Jishu/Power Syst. Technol.* **2021**, *45*, 825–832. [CrossRef]
5. Liu, T.B.; Zhang, J.; Xie, Y.B.; Zhang, J.K. Fault Feature Mining and Identification Method of 10kV XLPE Cable Combining SAE and RF. *Recent Adv. Electr. Electron. Eng.* **2025**, *18*, 589–599. [CrossRef]
6. Huang, J.T.; Zhou, K.; Xu, Y.F.; Meng, P.F.; Tang, Z.R.; Liang, Z.Y. Upper Sweeping Frequency Selection for Cable Defect Location Based on STFT. *IEEE Trans. Instrum. Meas.* **2023**, *72*, 3271718. [CrossRef]
7. Govindarajan, S.; Morales, A.; Ardila-Rey, J.A.; Purushothaman, N. A review on partial discharge diagnosis in cables: Theory, techniques, and trends. *Measurement* **2023**, *216*, 112882. [CrossRef]

8. Abu Bakar, A.; Yii, C.C.; Fern, C.K.; Pin, Y.H.; Lago, H.; Rohani, M. A Comparison of Double-End Partial Discharge Localization Algorithms in Power Cables. *Energies* **2023**, *16*, 1817. [CrossRef]
9. Yang, Y.; Shi, H.; Li, C.; Yang, S.; Wang, Y. Application of Artificial Intelligence in Partial Discharge Diagnosis of Power Cables: Research Progress. *High Volt. Technol.* **2025**, 1–19. [CrossRef]
10. Li, J.; Han, X.; Wang, H.; Zhou, Y.; Chen, H.; Guo, R.; Si, W. A Review of Partial Discharge Detection Technologies for Electrical Equipment: 2015–2025. *High Volt. Technol.* **2025**, *51*, 3132–3158. [CrossRef]
11. Li, W.; Bai, H.; Wu, W.; Yang, L.; Zhu, K.; Zhang, R.; Zhao, L. Evaluation of Insulation Aging and Fault Location of Power Cables Based on Oscillating Wave Partial Discharge Detection. *Electr. Meas. Instrum.* **2021**, *58*, 147–151. [CrossRef]
12. Guo, C.; Zhang, L.; Qian, Y.; Huang, C.; Yao, L.; Jiang, X. Research Status of Partial Discharge Detection and Localization Technology in XLPE Power Cables. *High Volt. Appar.* **2009**, *45*, 56–60. [CrossRef]
13. Zheng, H.; Cai, Q.S.; Zheng, J.S.; Zhen, Z.M.; Zou, W.; Chen, J.P. Quantitative Method for Ultrasonic Testing of Lead Seal Defects in High Voltage Cable Accessories. *IEEE Access* **2025**, *13*, 76047–76057. [CrossRef]
14. Yücel, M.K.; Legg, M.; Kappatos, V.; Gan, T.H. An ultrasonic guided wave approach for the inspection of overhead transmission line cables. *Appl. Acoust.* **2017**, *122*, 23–34. [CrossRef]
15. Deng, K.; Wen, Q.; Zhang, Y. Partial Discharge Defect Detection Method for Cable Terminals Based on Ultrasonic and Infrared Thermography. *Infrared Technol.* **2022**, *44*, 972–978.
16. Li, C.; Liu, J.; Liu, X.; Guo, L.; Liu, X. Analysis of Common Defects in Power Cables Based on X-ray Detection. *Electron. Test.* **2020**, *1*, 116–117. [CrossRef]
17. Chen, Y.; Sun, J.; Xu, Y.; Zhang, J. Research and Application of Fire Blocking Detection for Power Cables Based on Acoustic Localization Technology. *Electron. Technol. Softw. Eng.* **2022**, *22*, 106–109. [CrossRef]
18. Rahman, M.S.U.; Abou-Khousa, M.A.; Akbar, M.F. A review on microwave non-destructive testing (NDT) of composites. *Eng. Sci. Technol.—Int. J.—Jestech* **2024**, *58*, 101848. [CrossRef]
19. Cheng, L.; Xu, W.L.; Wang, X.Y.; Yang, L.J.; Liao, R.J.; Nie, Y.J. Defect Detection of Cable Termination Based on the Microwave Reflection Method. *IEEE Trans. Dielectr. Electr. Insul.* **2024**, *31*, 111–120. [CrossRef]
20. Balakrishnan, S.A.; Ramalingam, V.S.; Sundarsingh, E.F.; Anbalagan, A.; Ramachandran, A.; Ahmed, W.; Raman, S.; Praveen, R. Detection and characterisation of defects in composite materials using microwave non-destructive testing methods. *Proc. Inst. Mech. Eng. Part C—J. Mech. Eng. Sci.* **2024**, *238*, 7652–7660. [CrossRef]
21. Wang, X.; Wang, S.; Chen, J.; Jiang, J.; Li, P.; Wu, T. Corrosion Detection of Reinforced Concrete in Transmission and Transformation Power Systems Based on Microwave Reflection Method. *Zhejiang Electr. Power* **2022**, *41*, 62–67. [CrossRef]
22. Wang, L.; Li, A.; Cheng, L.; Hu, X.; Yang, J.; Chen, W. Nondestructive Testing Method for Composite Insulators Based on Microwave Reflection Technique. *High Volt. Eng.* **2015**, *41*, 584–591. [CrossRef]
23. Wang, L.; Li, A.; Cheng, L. Key Factors in the Microwave Nondestructive Testing Method for Composite Insulators. *High Volt. Eng.* **2017**, *43*, 203–209. [CrossRef]
24. Yang, X.; Yi, Z. *Fundamentals of Microwave Technology*, 3rd ed.; Tsinghua University Press: Beijing, China, 2021; pp. 55–69.

https://doi.org/10.3390/en19020499